Automatic Variational Inference in Stan

Alp Kucukelbir
Columbia University
alp@cs.columbia.edu

Rajesh Ranganath
Princeton University
rajeshr@cs.princeton.edu

Andrew Gelman
Columbia University
gelman@stat.columbia.edu

David M. Blei
Columbia University
david.blei@columbia.edu

Abstract

Variational inference is a scalable technique for approximate Bayesian inference. Deriving variational inference algorithms requires tedious model-specific calculations; this makes it difficult for non-experts to use. We propose an automatic variational inference algorithm, automatic differentiation variational inference (ADVI); we implement it in Stan (code available), a probabilistic programming system. In ADVI the user provides a Bayesian model and a dataset, nothing else. We make no conjugacy assumptions and support a broad class of models. The algorithm automatically determines an appropriate variational family and optimizes the variational objective. We compare ADVI to MCMC sampling across hierarchical generalized linear models, nonconjugate matrix factorization, and a mixture model. We train the mixture model on a quarter million images. With ADVI we can use variational inference on any model we write in Stan.

1 Introduction

Bayesian inference is a powerful framework for analyzing data. We design a model for data using latent variables; we then analyze data by calculating the posterior density of the latent variables. For machine learning models, calculating the posterior is often difficult; we resort to approximation.

Variational inference (VI) approximates the posterior with a simpler distribution [1, 2]. We search over a family of simple distributions and find the member closest to the posterior. This turns approximate inference into optimization. VI has had a tremendous impact on machine learning; it is typically faster than Markov chain Monte Carlo (MCMC) sampling (as we show here too) and has recently scaled up to massive data [3].

Unfortunately, VI algorithms are difficult to derive. We must first define the family of approximating distributions, and then calculate model-specific quantities relative to that family to solve the variational optimization problem. Both steps require expert knowledge. The resulting algorithm is tied to both the model and the chosen approximation.

In this paper we develop a method for automating variational inference, automatic differentiation variational inference (ADVI). Given any model from a wide class (specifically, probability models differentiable with respect to their latent variables), ADVI determines an appropriate variational family and an algorithm for optimizing the corresponding variational objective. We implement ADVI in Stan [4], a flexible probabilistic programming system. Stan describes a high-level language to define probabilistic models (e.g., Figure 2) as well as a model compiler, a library of transformations, and an efficient automatic differentiation toolbox. With ADVI we can now use variational inference on any model we write in Stan.[1] (See Appendices F to J.)

---

[1] ADVI is available in Stan 2.8. See Appendix C.

(a) Subset of 1000 images
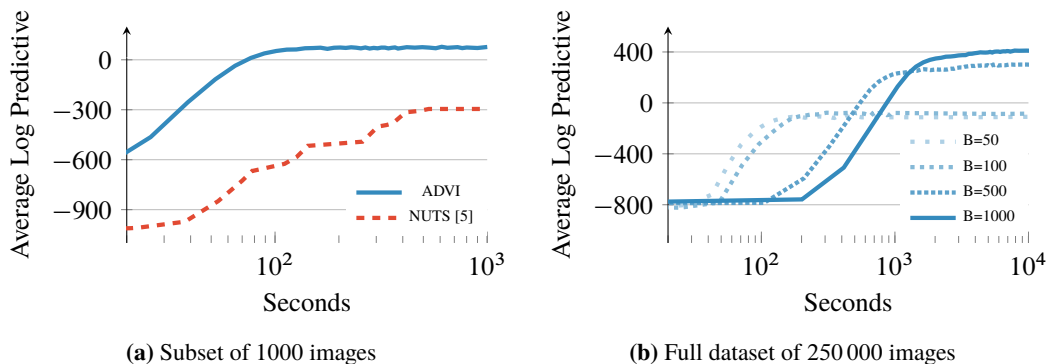
(b) Full dataset of 250 000 images

Figure 1: Held-out predictive accuracy results | Gaussian mixture model (GMM) of the imageCLEF image histogram dataset. **(a)** ADVI outperforms the no-U-turn sampler (NUTS), the default sampling method in Stan [5]. **(b)** ADVI scales to large datasets by subsampling minibatches of size B from the dataset at each iteration [3]. We present more details in Section 3.3 and Appendix J.

Figure 1 illustrates the advantages of our method. Consider a nonconjugate Gaussian mixture model for analyzing natural images; this is 40 lines in Stan (Figure 10). Figure 1a illustrates Bayesian inference on 1000 images. The y-axis is held-out likelihood, a measure of model fitness; the x-axis is time on a log scale. ADVI is orders of magnitude faster than NUTS, a state-of-the-art MCMC algorithm (and Stan's default inference technique) [5]. We also study nonconjugate factorization models and hierarchical generalized linear models in Section 3.

Figure 1b illustrates Bayesian inference on 250 000 images, the size of data we more commonly find in machine learning. Here we use ADVI with stochastic variational inference [3], giving an approximate posterior in under two hours. For data like these, MCMC techniques cannot complete the analysis.

Related work. ADVI automates variational inference within the Stan probabilistic programming system [4]. This draws on two major themes.

The first is a body of work that aims to generalize VI. Kingma and Welling [6] and Rezende et al. [7] describe a reparameterization of the variational problem that simplifies optimization. Ranganath et al. [8] and Salimans and Knowles [9] propose a black-box technique, one that only requires the model and the gradient of the approximating family. Titsias and Lázaro-Gredilla [10] leverage the gradient of the joint density for a small class of models. Here we build on and extend these ideas to automate variational inference; we highlight technical connections as we develop the method.

The second theme is probabilistic programming. Wingate and Weber [11] study VI in general probabilistic programs, as supported by languages like Church [12], Venture [13], and Anglican [14]. Another probabilistic programming system is infer.NET, which implements variational message passing [15], an efficient algorithm for conditionally conjugate graphical models. Stan supports a more comprehensive class of nonconjugate models with differentiable latent variables; see Section 2.1.

2   Automatic Differentiation Variational Inference

Automatic differentiation variational inference (ADVI) follows a straightforward recipe. First we transform the support of the latent variables to the real coordinate space. For example, the logarithm transforms a positive variable, such as a standard deviation, to the real line. Then we posit a Gaussian variational distribution to approximate the posterior. This induces a non-Gaussian approximation in the original variable space. Last we combine automatic differentiation with stochastic optimization to maximize the variational objective. We begin by defining the class of models we support.

2.1   Differentiable Probability Models

Consider a dataset $\mathbf{X} = \boldsymbol{x}_{1:N}$ with N observations. Each $\boldsymbol{x}_n$ is a discrete or continuous random vector. The likelihood $p(\mathbf{X} \mid \boldsymbol{\theta})$ relates the observations to a set of latent random variables $\boldsymbol{\theta}$. Bayesian
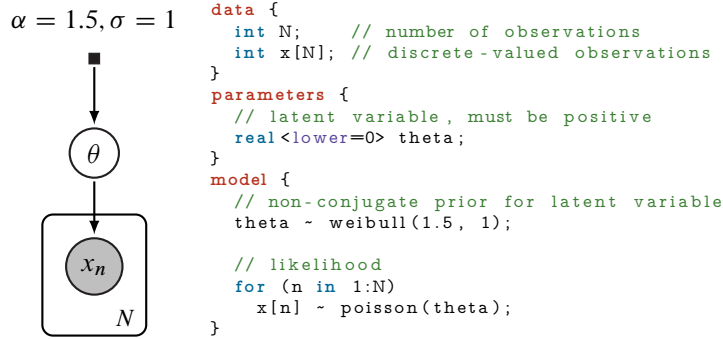
Figure 2: Specifying a simple nonconjugate probability model in Stan.

analysis posits a prior density $p(\boldsymbol{\theta})$ on the latent variables. Combining the likelihood with the prior gives the joint density $p(\mathbf{X}, \boldsymbol{\theta}) = p(\mathbf{X} \mid \boldsymbol{\theta}) \, p(\boldsymbol{\theta})$.

We focus on approximate inference for differentiable probability models. These models have continuous latent variables $\boldsymbol{\theta}$. They also have a gradient of the log-joint with respect to the latent variables $\nabla_{\boldsymbol{\theta}} \log p(\mathbf{X}, \boldsymbol{\theta})$. The gradient is valid within the support of the prior $\operatorname{supp}(p(\boldsymbol{\theta})) = \big\{ \boldsymbol{\theta} \mid \boldsymbol{\theta} \in \mathbb{R}^K \text{ and } p(\boldsymbol{\theta}) > 0 \big\} \subseteq \mathbb{R}^K$, where K is the dimension of the latent variable space. We assume that the support of the posterior equals that of the prior. We make no assumptions about conjugacy, either full or conditional.[2]

For example, consider a model that contains a Poisson likelihood with unknown rate, $p(x \mid \theta)$. The observed variable x is discrete; the latent rate θ is continuous and positive. Place a Weibull prior on θ, defined over the positive real numbers. The resulting joint density describes a nonconjugate differentiable probability model. (See Figure 2.) Its partial derivative $\partial / \partial\theta \; p(x, \theta)$ is valid within the support of the Weibull distribution, $\operatorname{supp}(p(\theta)) = \mathbb{R}^+ \subset \mathbb{R}$. Because this model is nonconjugate, the posterior is not a Weibull distribution. This presents a challenge for classical variational inference. In Section 2.3, we will see how ADVI handles this model.

Many machine learning models are differentiable. For example: linear and logistic regression, matrix factorization with continuous or discrete measurements, linear dynamical systems, and Gaussian processes. Mixture models, hidden Markov models, and topic models have discrete random variables. Marginalizing out these discrete variables renders these models differentiable. (We show an example in Section 3.3.) However, marginalization is not tractable for all models, such as the Ising model, sigmoid belief networks, and (untruncated) Bayesian nonparametric models.

2.2 Variational Inference

Bayesian inference requires the posterior density $p(\boldsymbol{\theta} \mid \mathbf{X})$, which describes how the latent variables vary when conditioned on a set of observations $\mathbf{X}$. Many posterior densities are intractable because their normalization constants lack closed forms. Thus, we seek to approximate the posterior.

Consider an approximating density $q(\boldsymbol{\theta} \, ; \, \boldsymbol{\phi})$ parameterized by $\boldsymbol{\phi}$. We make no assumptions about its shape or support. We want to find the parameters of $q(\boldsymbol{\theta} \, ; \, \boldsymbol{\phi})$ to best match the posterior according to some loss function. Variational inference (VI) minimizes the Kullback-Leibler (KL) divergence from the approximation to the posterior [2],

$$\boldsymbol{\phi}^* = \arg\min_{\boldsymbol{\phi}} \operatorname{KL}(q(\boldsymbol{\theta} \, ; \, \boldsymbol{\phi}) \, \| \, p(\boldsymbol{\theta} \mid \mathbf{X})). \tag{1}$$

Typically the KL divergence also lacks a closed form. Instead we maximize the evidence lower bound (ELBO), a proxy to the KL divergence,

$$\mathcal{L}(\boldsymbol{\phi}) = \mathbb{E}_{q(\boldsymbol{\theta})}\big[\log p(\mathbf{X}, \boldsymbol{\theta}) \big] - \mathbb{E}_{q(\boldsymbol{\theta})}\big[\log q(\boldsymbol{\theta} \, ; \, \boldsymbol{\phi}) \big].$$

The first term is an expectation of the joint density under the approximation, and the second is the entropy of the variational density. Maximizing the ELBO minimizes the KL divergence [1, 16].

---

[2] The posterior of a *fully* conjugate model is in the same family as the prior; a *conditionally* conjugate model has this property within the complete conditionals of the model [3].

The minimization problem from Eq. (1) becomes

$$\boldsymbol{\phi}^* = \arg\max_{\boldsymbol{\phi}} \mathcal{L}(\boldsymbol{\phi}) \quad \text{such that} \quad \text{supp}(q(\boldsymbol{\theta}\,;\,\boldsymbol{\phi})) \subseteq \text{supp}(p(\boldsymbol{\theta}\mid\mathbf{X})). \qquad (2)$$

We explicitly specify the support-matching constraint implied in the KL divergence.[3] We highlight this constraint, as we do not specify the form of the variational approximation; thus $q(\boldsymbol{\theta}\,;\,\boldsymbol{\phi})$ must remain within the support of the posterior, which we assume equal to the support of the prior.

Why is VI difficult to automate? In classical variational inference, we typically design a conditionally conjugate model. Then the optimal approximating family matches the prior. This satisfies the support constraint by definition [16]. When we want to approximate models that are not conditionally conjugate, we carefully study the model and design custom approximations. These depend on the model and on the choice of the approximating density.

One way to automate VI is to use black-box variational inference [8, 9]. If we select a density whose support matches the posterior, then we can directly maximize the ELBO using Monte Carlo (MC) integration and stochastic optimization. Another strategy is to restrict the class of models and use a fixed variational approximation [10]. For instance, we may use a Gaussian density for inference in unrestrained differentiable probability models, i.e. where $\text{supp}(p(\boldsymbol{\theta})) = \mathbb{R}^K$.

We adopt a transformation-based approach. First we automatically transform the support of the latent variables in our model to the real coordinate space. Then we posit a Gaussian variational density. The transformation induces a non-Gaussian approximation in the original variable space and guarantees that it stays within the support of the posterior. Here is how it works.

2.3 Automatic Transformation of Constrained Variables

Begin by transforming the support of the latent variables $\boldsymbol{\theta}$ such that they live in the real coordinate space $\mathbb{R}^K$. Define a one-to-one differentiable function $T : \text{supp}(p(\boldsymbol{\theta})) \rightarrow \mathbb{R}^K$ and identify the transformed variables as $\boldsymbol{\zeta} = T(\boldsymbol{\theta})$. The transformed joint density $g(\mathbf{X}, \boldsymbol{\zeta})$ is

$$g(\mathbf{X}, \boldsymbol{\zeta}) = p\big(\mathbf{X}, T^{-1}(\boldsymbol{\zeta})\big)\big|\det J_{T^{-1}}(\boldsymbol{\zeta})\big|,$$

where p is the joint density in the original latent variable space, and $J_{T^{-1}}$ is the Jacobian of the inverse of T. Transformations of continuous probability densities require a Jacobian; it accounts for how the transformation warps unit volumes [17]. (See Appendix D.)

Consider again our running example. The rate θ lives in $\mathbb{R}^+$. The logarithm $\zeta = T(\theta) = \log(\theta)$ transforms $\mathbb{R}^+$ to the real line $\mathbb{R}$. Its Jacobian adjustment is the derivative of the inverse of the logarithm, $|\det J_{T^{-1}(\zeta)}| = \exp(\zeta)$. The transformed density is

$$g(x, \zeta) = \text{Poisson}(x \mid \exp(\zeta))\, \text{Weibull}(\exp(\zeta)\,;\, 1.5, 1)\, \exp(\zeta).$$

Figures 3a and 3b depict this transformation.

As we describe in the introduction, we implement our algorithm in Stan to enable generic inference. Stan implements a model compiler that automatically handles transformations. It works by applying a library of transformations and their corresponding Jacobians to the joint model density.[4] This transforms the joint density of any differentiable probability model to the real coordinate space. Now we can choose a variational distribution independent from the model.

2.4 Implicit Non-Gaussian Variational Approximation

After the transformation, the latent variables $\boldsymbol{\zeta}$ have support on $\mathbb{R}^K$. We posit a diagonal (mean-field) Gaussian variational approximation

$$q(\boldsymbol{\zeta}\,;\,\boldsymbol{\phi}) = \mathcal{N}(\boldsymbol{\zeta}\,;\,\boldsymbol{\mu}, \boldsymbol{\sigma}) = \prod_{k=1}^{K} \mathcal{N}(\zeta_k\,;\,\mu_k, \sigma_k).$$

---

[3]If $\text{supp}(q) \not\subseteq \text{supp}(p)$ then outside the support of p we have $\text{KL}(q \parallel p) = \mathbb{E}_q[\log q] - \mathbb{E}_q[\log p] = -\infty$.
[4]Stan provides transformations for upper and lower bounds, simplex and ordered vectors, and structured matrices such as covariance matrices and Cholesky factors [4].
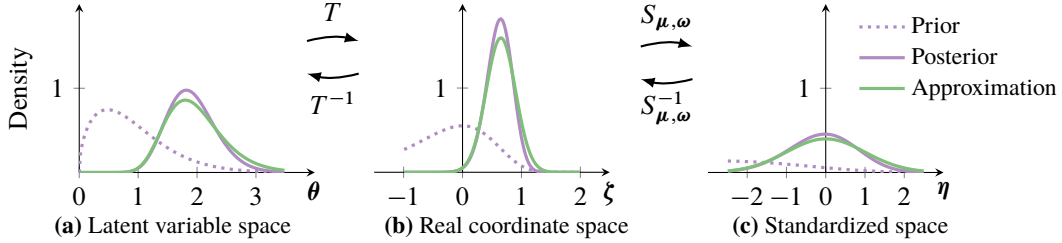
Figure 3: Transformations for ADVI. The purple line is the posterior. The green line is the approximation. **(a)** The latent variable space is $\mathbb{R}^+$. **(a→b)** T transforms the latent variable space to $\mathbb{R}$. **(b)** The variational approximation is a Gaussian. **(b→c)** $S_{\boldsymbol{\mu},\boldsymbol{\omega}}$ absorbs the parameters of the Gaussian. **(c)** We maximize the ELBO in the standardized space, with a fixed standard Gaussian approximation.

The vector $\boldsymbol{\phi} = (\mu_1, \cdots, \mu_K, \sigma_1, \cdots, \sigma_K)$ contains the mean and standard deviation of each Gaussian factor. This defines our variational approximation in the real coordinate space. (Figure 3b.)

The transformation T maps the support of the latent variables to the real coordinate space; its inverse T^{-1} maps back to the support of the latent variables. This implicitly defines the variational approximation in the original latent variable space as $q(T(\boldsymbol{\theta}) ; \boldsymbol{\phi}) \big| \det J_T(\boldsymbol{\theta}) \big|$. The transformation ensures that the support of this approximation is always bounded by that of the true posterior in the original latent variable space (Figure 3a). Thus we can freely optimize the ELBO in the real coordinate space (Figure 3b) without worrying about the support matching constraint.

The ELBO in the real coordinate space is

$$\mathcal{L}(\boldsymbol{\mu}, \boldsymbol{\sigma}) = \mathbb{E}_{q(\boldsymbol{\zeta})}\left[\log p\big(\mathbf{X}, T^{-1}(\boldsymbol{\zeta})\big) + \log \big| \det J_{T^{-1}}(\boldsymbol{\zeta}) \big| \right] + \frac{K}{2}\left(1 + \log(2\pi)\right) + \sum_{k=1}^{K} \log \sigma_k,$$

where we plug in the analytic form of the Gaussian entropy. (The derivation is in Appendix A.)

We choose a diagonal Gaussian for efficiency. This choice may call to mind the Laplace approximation technique, where a second-order Taylor expansion around the maximum-a-posteriori estimate gives a Gaussian approximation to the posterior. However, using a Gaussian variational approximation is not equivalent to the Laplace approximation [18]. The Laplace approximation relies on maximizing the probability density; it fails with densities that have discontinuities on its boundary. The Gaussian approximation considers probability mass; it does not suffer this degeneracy. Furthermore, our approach is distinct in another way: because of the transformation, the posterior approximation in the original latent variable space (Figure 3a) is non-Gaussian.

2.5 Automatic Differentiation for Stochastic Optimization

We now maximize the ELBO in real coordinate space,

$$\boldsymbol{\mu}^*, \boldsymbol{\sigma}^* = \arg\max_{\boldsymbol{\mu}, \boldsymbol{\sigma}} \mathcal{L}(\boldsymbol{\mu}, \boldsymbol{\sigma}) \quad \text{such that} \quad \boldsymbol{\sigma} \succ 0. \tag{3}$$

We use gradient ascent to reach a local maximum of the ELBO. Unfortunately, we cannot apply automatic differentiation to the ELBO in this form. This is because the expectation defines an intractable integral that depends on $\boldsymbol{\mu}$ and $\boldsymbol{\sigma}$; we cannot directly represent it as a computer program. Moreover, the standard deviations in $\boldsymbol{\sigma}$ must remain positive. Thus, we employ one final transformation: elliptical standardization[5] [19], shown in Figures 3b and 3c.

First re-parameterize the Gaussian distribution with the log of the standard deviation, $\boldsymbol{\omega} = \log(\boldsymbol{\sigma})$, applied element-wise. The support of $\boldsymbol{\omega}$ is now the real coordinate space and $\boldsymbol{\sigma}$ is always positive. Then define the standardization $\boldsymbol{\eta} = S_{\boldsymbol{\mu},\boldsymbol{\omega}}(\boldsymbol{\zeta}) = \mathrm{diag}\big(\exp(\boldsymbol{\omega})^{-1}\big)(\boldsymbol{\zeta} - \boldsymbol{\mu})$. The standardization

---

[5]Also known as a "co-ordinate transformation" [7], an "invertible transformation" [10], and the "reparameterization trick" [6].

Algorithm 1: Automatic differentiation variational inference (ADVI)

Input: Dataset $\mathbf{X} = \boldsymbol{x}_{1:N}$, model $p(\mathbf{X}, \boldsymbol{\theta})$.
Set iteration counter $i = 0$ and choose a stepsize sequence $\boldsymbol{\rho}^{(i)}$.
Initialize $\boldsymbol{\mu}^{(0)} = \mathbf{0}$ and $\boldsymbol{\omega}^{(0)} = \mathbf{0}$.

while *change in* ELBO *is above some threshold* **do**

    Draw M samples $\boldsymbol{\eta}_m \sim \mathcal{N}(\mathbf{0}, \mathbf{I})$ from the standard multivariate Gaussian.

    Invert the standardization $\boldsymbol{\zeta}_m = \mathrm{diag}(\exp(\boldsymbol{\omega}^{(i)}))\boldsymbol{\eta}_m + \boldsymbol{\mu}^{(i)}$.

    Approximate $\nabla_{\boldsymbol{\mu}}\mathcal{L}$ and $\nabla_{\boldsymbol{\omega}}\mathcal{L}$ using MC integration (Eqs. (4) and (5)).

    Update $\boldsymbol{\mu}^{(i+1)} \longleftarrow \boldsymbol{\mu}^{(i)} + \boldsymbol{\rho}^{(i)}\nabla_{\boldsymbol{\mu}}\mathcal{L}$ and $\boldsymbol{\omega}^{(i+1)} \longleftarrow \boldsymbol{\omega}^{(i)} + \boldsymbol{\rho}^{(i)}\nabla_{\boldsymbol{\omega}}\mathcal{L}$.

    Increment iteration counter.

end
Return $\boldsymbol{\mu}^* \longleftarrow \boldsymbol{\mu}^{(i)}$ and $\boldsymbol{\omega}^* \longleftarrow \boldsymbol{\omega}^{(i)}$.

---

encapsulates the variational parameters and gives the fixed density

$$q(\boldsymbol{\eta}\,;\,\mathbf{0}, \mathbf{I}) = \mathcal{N}(\boldsymbol{\eta}\,;\,\mathbf{0}, \mathbf{I}) = \prod_{k=1}^{K} \mathcal{N}(\eta_k\,;\,0, 1).$$

The standardization transforms the variational problem from Eq. (3) into

$$\boldsymbol{\mu}^*, \boldsymbol{\omega}^* = \underset{\boldsymbol{\mu},\boldsymbol{\omega}}{\arg\max}\ \mathcal{L}(\boldsymbol{\mu}, \boldsymbol{\omega})$$

$$= \underset{\boldsymbol{\mu},\boldsymbol{\omega}}{\arg\max}\ \mathbb{E}_{\mathcal{N}(\boldsymbol{\eta}\,;\,\mathbf{0},\mathbf{I})}\left[\log p\big(\mathbf{X}, T^{-1}(S_{\boldsymbol{\mu},\boldsymbol{\omega}}^{-1}(\boldsymbol{\eta}))\big) + \log\big|\det J_{T^{-1}}\big(S_{\boldsymbol{\mu},\boldsymbol{\omega}}^{-1}(\boldsymbol{\eta})\big)\big| \right] + \sum_{k=1}^{K}\omega_k,$$

where we drop constant terms from the calculation. This expectation is with respect to a standard Gaussian and the parameters $\boldsymbol{\mu}$ and $\boldsymbol{\omega}$ are both unconstrained (Figure 3c). We push the gradient inside the expectations and apply the chain rule to get

$$\nabla_{\boldsymbol{\mu}}\mathcal{L} = \mathbb{E}_{\mathcal{N}(\boldsymbol{\eta})}\left[\nabla_{\boldsymbol{\theta}} \log p(\mathbf{X}, \boldsymbol{\theta})\nabla_{\boldsymbol{\zeta}} T^{-1}(\boldsymbol{\zeta}) + \nabla_{\boldsymbol{\zeta}} \log\big|\det J_{T^{-1}}(\boldsymbol{\zeta})\big| \right], \tag{4}$$

$$\nabla_{\omega_k}\mathcal{L} = \mathbb{E}_{\mathcal{N}(\eta_k)}\left[\big(\nabla_{\theta_k} \log p(\mathbf{X}, \boldsymbol{\theta})\nabla_{\zeta_k} T^{-1}(\boldsymbol{\zeta}) + \nabla_{\zeta_k} \log\big|\det J_{T^{-1}}(\boldsymbol{\zeta})\big|\big) \eta_k \exp(\omega_k) \right] + 1. \tag{5}$$

(The derivations are in Appendix B.)

We can now compute the gradients inside the expectation with automatic differentiation. The only thing left is the expectation. MC integration provides a simple approximation: draw M samples from the standard Gaussian and evaluate the empirical mean of the gradients within the expectation [20].

This gives unbiased noisy gradients of the ELBO for any differentiable probability model. We can now use these gradients in a stochastic optimization routine to automate variational inference.

2.6 Automatic Variational Inference

Equipped with unbiased noisy gradients of the ELBO, ADVI implements stochastic gradient ascent (Algorithm 1). We ensure convergence by choosing a decreasing step-size sequence. In practice, we use an adaptive sequence [21] with finite memory. (See Appendix E for details.)

ADVI has complexity $\mathcal{O}(NMK)$ per iteration, where M is the number of MC samples (typically between 1 and 10). Coordinate ascent VI has complexity $\mathcal{O}(NK)$ per pass over the dataset. We scale ADVI to large datasets using stochastic optimization [3, 10]. The adjustment to Algorithm 1 is simple: sample a minibatch of size $B \ll N$ from the dataset and scale the likelihood of the sampled minibatch by N/B [3]. The stochastic extension of ADVI has per-iteration complexity $\mathcal{O}(BMK)$.
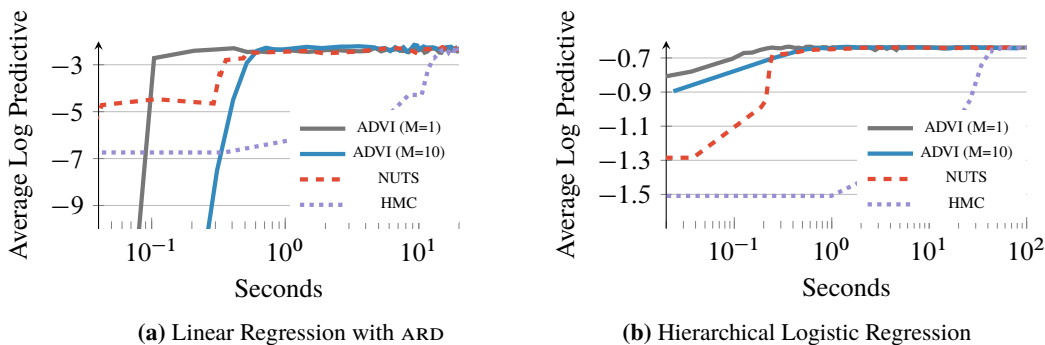
(a) Linear Regression with ARD

(b) Hierarchical Logistic Regression

Figure 4: Hierarchical generalized linear models. Comparison of ADVI to MCMC: held-out predictive likelihood as a function of wall time.

3 Empirical Study

We now study ADVI across a variety of models. We compare its speed and accuracy to two Markov chain Monte Carlo (MCMC) sampling algorithms: Hamiltonian Monte Carlo (HMC) [22] and the no-U-turn sampler (NUTS)[6] [5]. We assess ADVI convergence by tracking the ELBO. To place ADVI and MCMC on a common scale, we report predictive likelihood on held-out data as a function of time. We approximate the posterior predictive likelihood using a MC estimate. For MCMC, we plug in posterior samples. For ADVI, we draw samples from the posterior approximation during the optimization. We initialize ADVI with a draw from a standard Gaussian.

We explore two hierarchical regression models, two matrix factorization models, and a mixture model. All of these models have nonconjugate prior structures. We conclude by analyzing a dataset of 250 000 images, where we report results across a range of minibatch sizes B.

3.1 A Comparison to Sampling: Hierarchical Regression Models

We begin with two nonconjugate regression models: linear regression with automatic relevance determination (ARD) [16] and hierarchical logistic regression [23].

Linear Regression with ARD. This is a sparse linear regression model with a hierarchical prior structure. (Details in Appendix F.) We simulate a dataset with 250 regressors such that half of the regressors have no predictive power. We use 10 000 training samples and hold out 1000 for testing.

Logistic Regression with Spatial Hierarchical Prior. This is a hierarchical logistic regression model from political science. The prior captures dependencies, such as states and regions, in a polling dataset from the United States 1988 presidential election [23]. (Details in Appendix G.) We train using 10 000 data points and withhold 1536 for evaluation. The regressors contain age, education, state, and region indicators. The dimension of the regression problem is 145.

Results. Figure 4 plots average log predictive accuracy as a function of time. For these simple models, all methods reach the same predictive accuracy. We study ADVI with two settings of M, the number of MC samples used to estimate gradients. A single sample per iteration is sufficient; it is also the fastest. (We set $M = 1$ from here on.)

3.2 Exploring Nonconjugacy: Matrix Factorization Models

We continue by exploring two nonconjugate non-negative matrix factorization models: a constrained Gamma Poisson model [24] and a Dirichlet Exponential model. Here, we show how easy it is to explore new models using ADVI. In both models, we use the Frey Face dataset, which contains 1956 frames (28×20 pixels) of facial expressions extracted from a video sequence.

Constrained Gamma Poisson. This is a Gamma Poisson factorization model with an ordering constraint: each row of the Gamma matrix goes from small to large values. (Details in Appendix H.)

---

[6]NUTS is an adaptive extension of HMC. It is the default sampler in Stan.

(a) Gamma Poisson Predictive Likelihood

(b) Dirichlet Exponential Predictive Likelihood

(c) Gamma Poisson Factors

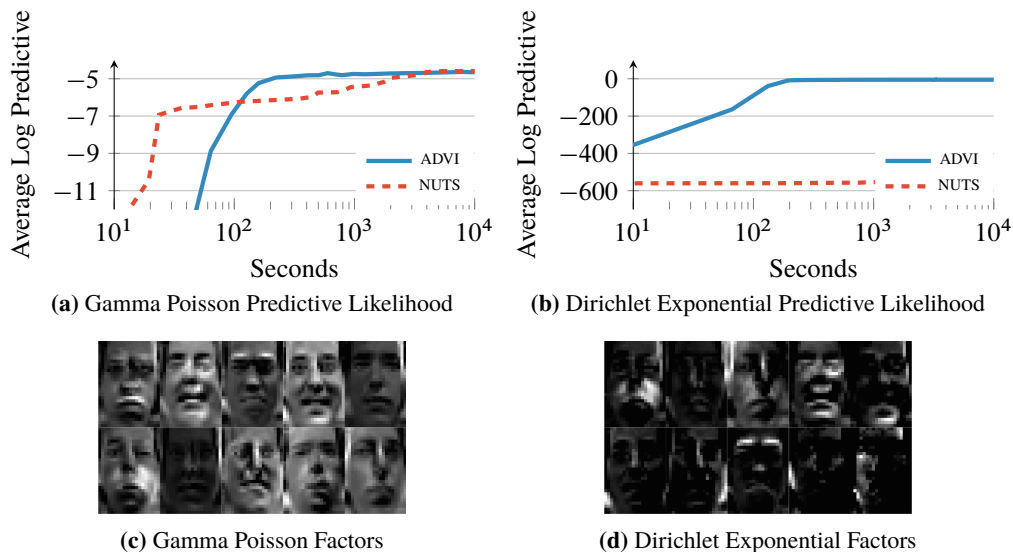**(d)** Dirichlet Exponential Factors

Figure 5: Non-negative matrix factorization of the Frey Faces dataset. Comparison of ADVI to MCMC: held-out predictive likelihood as a function of wall time.

Dirichlet Exponential. This is a nonconjugate Dirichlet Exponential factorization model with a Poisson likelihood. (Details in Appendix I.)

Results. Figure 5 shows average log predictive accuracy as well as ten factors recovered from both models. ADVI provides an order of magnitude speed improvement over NUTS (Figure 5a). NUTS struggles with the Dirichlet Exponential model (Figure 5b). In both cases, HMC does not produce any useful samples within a budget of one hour; we omit HMC from the plots.

3.3 Scaling to Large Datasets: Gaussian Mixture Model

We conclude with the Gaussian mixture model (GMM) example we highlighted earlier. This is a nonconjugate GMM applied to color image histograms. We place a Dirichlet prior on the mixture proportions, a Gaussian prior on the component means, and a lognormal prior on the standard deviations. (Details in Appendix J.) We explore the imageCLEF dataset, which has 250 000 images [25]. We withhold 10 000 images for evaluation.

In Figure 1a we randomly select 1000 images and train a model with 10 mixture components. NUTS struggles to find an adequate solution and HMC fails altogether. This is likely due to label switching, which can affect HMC-based techniques in mixture models [4].

Figure 1b shows ADVI results on the full dataset. Here we use ADVI with stochastic subsampling of minibatches from the dataset [3]. We increase the number of mixture components to 30. With a minibatch size of 500 or larger, ADVI reaches high predictive accuracy. Smaller minibatch sizes lead to suboptimal solutions, an effect also observed in [3]. ADVI converges in about two hours.

4 Conclusion

We develop automatic differentiation variational inference (ADVI) in Stan. ADVI leverages automatic transformations, an implicit non-Gaussian variational approximation, and automatic differentiation. This is a valuable tool. We can explore many models and analyze large datasets with ease. We emphasize that ADVI is currently available as part of Stan; it is ready for anyone to use.

References

[1] Michael I Jordan, Zoubin Ghahramani, Tommi S Jaakkola, and Lawrence K Saul. An introduction to variational methods for graphical models. *Machine Learning*, 37(2):183–233, 1999.

[2] Martin J Wainwright and Michael I Jordan. Graphical models, exponential families, and variational inference. *Foundations and Trends in Machine Learning*, 1(1-2):1–305, 2008.

[3] Matthew D Hoffman, David M Blei, Chong Wang, and John Paisley. Stochastic variational inference. *The Journal of Machine Learning Research*, 14(1):1303–1347, 2013.

[4] Stan Development Team. *Stan Modeling Language Users Guide and Reference Manual*, 2015.

[5] Matthew D Hoffman and Andrew Gelman. The No-U-Turn sampler. *The Journal of Machine Learning Research*, 15(1):1593–1623, 2014.

[6] Diederik Kingma and Max Welling. Auto-encoding variational Bayes. *arXiv:1312.6114*, 2013.

[7] Danilo J Rezende, Shakir Mohamed, and Daan Wierstra. Stochastic backpropagation and approximate inference in deep generative models. In *ICML*, pages 1278–1286, 2014.

[8] Rajesh Ranganath, Sean Gerrish, and David Blei. Black box variational inference. In *AISTATS*, pages 814–822, 2014.

[9] Tim Salimans and David Knowles. On using control variates with stochastic approximation for variational Bayes. *arXiv preprint arXiv:1401.1022*, 2014.

[10] Michalis Titsias and Miguel Lázaro-Gredilla. Doubly stochastic variational Bayes for non-conjugate inference. In *ICML*, pages 1971–1979, 2014.

[11] David Wingate and Theophane Weber. Automated variational inference in probabilistic programming. *arXiv preprint arXiv:1301.1299*, 2013.

[12] Noah D Goodman, Vikash K Mansinghka, Daniel Roy, Keith Bonawitz, and Joshua B Tenenbaum. Church: A language for generative models. In *UAI*, pages 220–229, 2008.

[13] Vikash Mansinghka, Daniel Selsam, and Yura Perov. Venture: a higher-order probabilistic programming platform with programmable inference. *arXiv:1404.0099*, 2014.

[14] Frank Wood, Jan Willem van de Meent, and Vikash Mansinghka. A new approach to probabilistic programming inference. In *AISTATS*, pages 2–46, 2014.

[15] John M Winn and Christopher M Bishop. Variational message passing. In *Journal of Machine Learning Research*, pages 661–694, 2005.

[16] Christopher M Bishop. *Pattern Recognition and Machine Learning*. Springer New York, 2006.

[17] David J Olive. *Statistical Theory and Inference*. Springer, 2014.

[18] Manfred Opper and Cédric Archambeau. The variational Gaussian approximation revisited. *Neural computation*, 21(3):786–792, 2009.

[19] Wolfgang Härdle and Léopold Simar. *Applied multivariate statistical analysis*. Springer, 2012.

[20] Christian P Robert and George Casella. *Monte Carlo statistical methods*. Springer, 1999.

[21] John Duchi, Elad Hazan, and Yoram Singer. Adaptive subgradient methods for online learning and stochastic optimization. *The Journal of Machine Learning Research*, 12:2121–2159, 2011.

[22] Mark Girolami and Ben Calderhead. Riemann manifold langevin and hamiltonian monte carlo methods. *Journal of the Royal Statistical Society: Series B*, 73(2):123–214, 2011.

[23] Andrew Gelman and Jennifer Hill. *Data analysis using regression and multilevel/hierarchical models*. Cambridge University Press, 2006.

[24] John Canny. GaP: a factor model for discrete data. In *ACM SIGIR*, pages 122–129. ACM, 2004.

[25] Mauricio Villegas, Roberto Paredes, and Bart Thomee. Overview of the ImageCLEF 2013 Scalable Concept Image Annotation Subtask. In *CLEF Evaluation Labs and Workshop*, 2013.

A   Transformation of the Evidence Lower Bound

Recall that $\boldsymbol{\zeta} = T(\boldsymbol{\theta})$ and that the variational approximation in the real coordinate space is $q(\boldsymbol{\zeta}\,;\boldsymbol{\phi})$.

We begin with the evidence lower bound (ELBO) in the original latent variable space. We then transform the latent variable space of to the real coordinate space.

$$
\begin{aligned}
\mathcal{L} &= \int q(\boldsymbol{\theta}\,;\boldsymbol{\phi}) \log\left[\frac{p(\mathbf{X},\boldsymbol{\theta})}{q(\boldsymbol{\theta}\,;\boldsymbol{\phi})}\right]\mathrm{d}\boldsymbol{\theta} \\
&= \int q(\boldsymbol{\zeta}\,;\boldsymbol{\phi}) \log\left[\frac{p\big(\mathbf{X},T^{-1}(\boldsymbol{\zeta})\big)\big|\det J_{T^{-1}}(\boldsymbol{\zeta})\big|}{q(\boldsymbol{\zeta}\,;\boldsymbol{\phi})}\right]\mathrm{d}\boldsymbol{\zeta} \\
&= \int q(\boldsymbol{\zeta}\,;\boldsymbol{\phi}) \log\left[p\big(\mathbf{X},T^{-1}(\boldsymbol{\zeta})\big)\big|\det J_{T^{-1}}(\boldsymbol{\zeta})\big|\right]\mathrm{d}\boldsymbol{\zeta} - \int q(\boldsymbol{\zeta}\,;\boldsymbol{\phi}) \log\left[q(\boldsymbol{\zeta}\,;\boldsymbol{\phi})\right]\mathrm{d}\boldsymbol{\zeta} \\
&= \mathbb{E}_{q(\boldsymbol{\zeta})}\left[\log p\big(\mathbf{X},T^{-1}(\boldsymbol{\zeta})\big) + \log\big|\det J_{T^{-1}}(\boldsymbol{\zeta})\big|\right] - \mathbb{E}_{q(\boldsymbol{\zeta})}\left[\log q(\boldsymbol{\zeta}\,;\boldsymbol{\phi})\right]
\end{aligned}
$$

The variational approximation in the real coordinate space is a Gaussian. Plugging in its entropy gives the ELBO in the real coordinate space

$$
\mathcal{L} = \mathbb{E}_{q(\boldsymbol{\zeta})}\left[\log p\big(\mathbf{X},T^{-1}(\boldsymbol{\zeta})\big) + \log\big|\det J_{T^{-1}}(\boldsymbol{\zeta})\big|\right] + \frac{1}{2}K\left(1+\log(2\pi)\right) + \sum_{k=1}^{K}\log\sigma_k.
$$

B   Gradients of the Evidence Lower Bound

First, consider the gradient with respect to the $\boldsymbol{\mu}$ parameter of the standardization. We exchange the order of the gradient and the integration through the dominated convergence theorem [1]. The rest is the chain rule for differentiation.

$$
\begin{aligned}
\nabla_{\boldsymbol{\mu}}\mathcal{L} &= \nabla_{\boldsymbol{\mu}}\Big\{\mathbb{E}_{\mathcal{N}(\boldsymbol{\eta}\,;\mathbf{0},\mathbf{I})}\left[\log p\big(\mathbf{X},T^{-1}(S_{\boldsymbol{\mu},\boldsymbol{\omega}}^{-1}(\boldsymbol{\eta}))\big) + \log\big|\det J_{T^{-1}}\big(S_{\boldsymbol{\mu},\boldsymbol{\omega}}^{-1}(\boldsymbol{\eta})\big)\big|\right] \\
&\qquad + \frac{K}{2}(1+\log(2\pi)) + \sum_{k=1}^{K}\log\sigma_k\Big\} \\
&= \mathbb{E}_{\mathcal{N}(\boldsymbol{\eta}\,;\mathbf{0},\mathbf{I})}\left[\nabla_{\boldsymbol{\mu}}\left\{\log p\big(\mathbf{X},T^{-1}(S^{-1}(\boldsymbol{\eta}))\big) + \log\big|\det J_{T^{-1}}\big(S^{-1}(\boldsymbol{\eta})\big)\big|\right\}\right] \\
&= \mathbb{E}_{\mathcal{N}(\boldsymbol{\eta}\,;\mathbf{0},\mathbf{I})}\left[\nabla_{\boldsymbol{\theta}}\log p(\mathbf{X},\boldsymbol{\theta})\nabla_{\boldsymbol{\zeta}}T^{-1}(\boldsymbol{\zeta})\nabla_{\boldsymbol{\mu}}S_{\boldsymbol{\mu},\boldsymbol{\omega}}^{-1}(\boldsymbol{\eta}) + \nabla_{\boldsymbol{\zeta}}\log\big|\det J_{T^{-1}}(\boldsymbol{\zeta})\big|\nabla_{\boldsymbol{\mu}}S_{\boldsymbol{\mu},\boldsymbol{\omega}}^{-1}(\boldsymbol{\eta})\right] \\
&= \mathbb{E}_{\mathcal{N}(\boldsymbol{\eta}\,;\mathbf{0},\mathbf{I})}\left[\nabla_{\boldsymbol{\theta}}\log p(\mathbf{X},\boldsymbol{\theta})\nabla_{\boldsymbol{\zeta}}T^{-1}(\boldsymbol{\zeta}) + \nabla_{\boldsymbol{\zeta}}\log\big|\det J_{T^{-1}}(\boldsymbol{\zeta})\big|\right]
\end{aligned}
$$

Similarly, consider the gradient with respect to the $\boldsymbol{\omega}$ parameter of the standardization. The gradient with respect to a single component, ω_k, has a clean form. We abuse the ∇ notation to maintain consistency with the rest of the text (instead of switching to ∂).

$$
\begin{aligned}
\nabla_{\omega_k}\mathcal{L} &= \nabla_{\omega_k}\Big\{\mathbb{E}_{\mathcal{N}(\boldsymbol{\eta}\,;\mathbf{0},\mathbf{I})}\left[\log p\big(\mathbf{X},T^{-1}(S_{\boldsymbol{\mu},\boldsymbol{\omega}}^{-1}(\boldsymbol{\eta}))\big) + \log\big|\det J_{T^{-1}}\big(S_{\boldsymbol{\mu},\boldsymbol{\omega}}^{-1}(\boldsymbol{\eta})\big)\big|\right] \\
&\qquad + \frac{K}{2}(1+\log(2\pi)) + \sum_{k=1}^{K}\log(\exp(\omega_k))\Big\} \\
&= \mathbb{E}_{\mathcal{N}(\eta_k)}\left[\nabla_{\omega_k}\left\{\log p\big(\mathbf{X},T^{-1}(S_{\boldsymbol{\mu},\boldsymbol{\omega}}^{-1}(\boldsymbol{\eta}))\big) + \log\big|\det J_{T^{-1}}\big(S_{\boldsymbol{\mu},\boldsymbol{\omega}}^{-1}(\boldsymbol{\eta})\big)\big|\right\}\right] + 1 \\
&= \mathbb{E}_{\mathcal{N}(\eta_k)}\left[\big(\nabla_{\theta_k}\log p(\mathbf{X},\boldsymbol{\theta})\nabla_{\zeta_k}T^{-1}(\boldsymbol{\zeta}) + \nabla_{\zeta_k}\log\big|\det J_{T^{-1}}(\boldsymbol{\zeta})\big|\big)\nabla_{\omega_k}S_{\boldsymbol{\mu},\boldsymbol{\omega}}^{-1}(\boldsymbol{\eta})\right] + 1. \\
&= \mathbb{E}_{\mathcal{N}(\eta_k)}\left[\big(\nabla_{\theta_k}\log p(\mathbf{X},\boldsymbol{\theta})\nabla_{\zeta_k}T^{-1}(\boldsymbol{\zeta}) + \nabla_{\zeta_k}\log\big|\det J_{T^{-1}}(\boldsymbol{\zeta})\big|\big)\eta_k\exp(\omega_k)\right] + 1.
\end{aligned}
$$

C   Running ADVI in Stan

Visit `http://mc-stan.org/` to download the latest version of Stan. Follow instructions on how to install Stan. You are then ready to use ADVI.

Stan offers multiple interfaces. We describe the command line interface (`cmdStan`) below.

The syntax is

```
./myModel    variational
             grad_samples=M              ( M = 1 default )
             data file=myData.data.R
             output file=output_advi.csv
             diagnostic_file=elbo_advi.csv
```

where `myData.data.R` is the dataset stored in the R language Rdump format. `output_advi.csv` contains samples from the posterior and `elbo_advi.csv` reports the ELBO.

D   Transformations of Continuous Probability Densities

We present a brief summary of transformations, largely based on [2].

Consider a univariate (scalar) random variable X with probability density function $f_X(x)$. Let $\mathcal{X} = \text{supp}(f_X(x))$ be the support of X. Now consider another random variable Y defined as $Y = T(X)$. Let $\mathcal{Y} = \text{supp}(f_Y(y))$ be the support of Y.

If T is a one-to-one and differentiable function from $\mathcal{X}$ to $\mathcal{Y}$, then Y has probability density function

$$f_Y(y) = f_X\big(T^{-1}(y)\big) \left| \frac{\mathrm{d}T^{-1}(y)}{\mathrm{d}y} \right|.$$

Let us sketch a proof. Consider the cumulative density function Y. If the transformation T is increasing, we directly apply its inverse to the cdf of Y. If the transformation T is decreasing, we apply its inverse to one minus the cdf of Y. The probability density function is the derivative of the cumulative density function. These things combined give the absolute value of the derivative above.

The extension to multivariate variables X and Y requires a multivariate version of the absolute value of the derivative of the inverse transformation. This is the the absolute determinant of the Jacobian, $|\det J_{T^{-1}}(Y)|$ where the Jacobian is

$$J_{T^{-1}}(Y) = \begin{pmatrix} \frac{\partial T_1^{-1}}{\partial y_1} & \cdots & \frac{\partial T_1^{-1}}{\partial y_K} \\ \vdots & & \vdots \\ \frac{\partial T_K^{-1}}{\partial y_1} & \cdots & \frac{\partial T_K^{-1}}{\partial y_K} \end{pmatrix}.$$

Intuitively, the Jacobian describes how a transformation warps unit volumes across spaces. This matters for transformations of random variables, since probability density functions must always integrate to one.

E   Setting a Stepsize Sequence for ADVI

We use adaGrad [3] to adaptively set the stepsize sequence in ADVI. While adaGrad offers attractive convergence properties, it can be slow for non-convex problems. One reason is because it has infinite memory. (It tracks the norm of the gradient starting from the beginning of the optimization.) In ADVI we randomly initialize the variational approximation, which can be far from the true posterior. This makes adaGrad take very small steps for the rest of the optimization, thus slowing convergence. Limiting adaGrad's memory speeds up convergence in practice, an effect also observed in training neural networks [4]. (See [5] for an analysis of these trade-offs and a method that combines benefits from both.)

Consider the stepsize $\boldsymbol{\rho}^{(i)}$ and a gradient vector $\boldsymbol{g}^{(i)}$ at iteration i. In adaGrad, kth element of $\boldsymbol{\rho}^{(i)}$ is

$$\rho_k^{(i)} = \frac{\eta}{\tau + \sqrt{s_k^{(i)}}}.$$

The vector $\boldsymbol{s}$ is the gradient vector squared element-wise and summed over all times steps since the start of the optimization. Instead, we limit this by recursively downweighting previous iterations as

$$s_k^{(i)} = 0.9 \times s_k^{(i-1)} + 0.1 \times g_k^{2\,(i)}.$$

We do a grid search for the scaling coefficient η and, following Hoffman et al. [6], set the offset $\tau = 1$.

F   Linear Regression with Automatic Relevance Determination

Linear regression with automatic relevance determination (ARD) is a high-dimensional sparse regression model [7, 8]. We describe the model below. Stan code is in Figure 6.

The inputs are $\mathbf{X} = \boldsymbol{x}_{1:N}$ where each $\boldsymbol{x}_n$ is D-dimensional. The outputs are $\boldsymbol{y} = y_{1:N}$ where each y_n is 1-dimensional. The weights vector $\boldsymbol{w}$ is D-dimensional. The likelihood

$$p(\boldsymbol{y} \mid \mathbf{X}, \boldsymbol{w}, \sigma) = \prod_{n=1}^{N} \mathcal{N}\left(y_n \mid \boldsymbol{w}^\top \boldsymbol{x}_n \,,\, \sigma\right)$$

describes measurements corrupted by iid Gaussian noise with unknown standard deviation σ.

The ARD prior and hyper-prior structure is as follows

$$p(\boldsymbol{w}, \sigma, \boldsymbol{\alpha}) = p(\boldsymbol{w}, \sigma \mid \boldsymbol{\alpha}) p(\boldsymbol{\alpha})$$

$$= \mathcal{N}\left(\boldsymbol{w} \mid 0 \,,\, \sigma\left(\operatorname{diag}\sqrt{\boldsymbol{\alpha}}\right)^{-1}\right) \operatorname{InvGam}(\sigma \mid a_0, b_0) \prod_{i=1}^{D} \operatorname{Gam}(\alpha_i \mid c_0, d_0)$$

where $\boldsymbol{\alpha}$ is a D-dimensional hyper-prior on the weights, where each component gets its own independent Gamma prior.

We simulate data such that only half the regressions have predictive power. The results in Figure 4a use $a_0 = b_0 = c_0 = d_0 = 1$ as hyper-parameters for the Gamma priors.

G   Hierarchical Logistic Regression

Hierarchical logistic regression models structured datasets in an intuitive way. We study a model of voting preferences from the 1988 United States presidential election. Chapter 14.1 of [9] motivates the model and explains the dataset. We also describe the model below. Stan code is in Figure 7, based on [10].

$$\Pr(y_n = 1) = \operatorname{sigmoid}\bigg(\beta^0 + \beta^{\text{female}} \cdot \text{female}_n + \beta^{\text{black}} \cdot \text{black}_n + \beta^{\text{female.black}} \cdot \text{female.black}_n$$

$$+ \alpha_{k[n]}^{\text{age}} + \alpha_{l[n]}^{\text{edu}} + \alpha_{k[n],l[n]}^{\text{age.edu}} + \alpha_{j[n]}^{\text{state}}\bigg)$$

$$\alpha_j^{\text{state}} \sim \mathcal{N}\left(\alpha_{m[j]}^{\text{region}} + \beta^{\text{v.prev}} \cdot \text{v.prev}_j \,,\, \sigma_{\text{state}}\right).$$

The hierarchical variables are

$$\alpha_k^{\text{age}} \sim \mathcal{N}\left(0 \,,\, \sigma_{\text{age}}\right) \text{ for } k = 1, \ldots, K$$

$$\alpha_l^{\text{edu}} \sim \mathcal{N}\left(0 \,,\, \sigma_{\text{edu}}\right) \text{ for } l = 1, \ldots, L$$

$$\alpha_{k,l}^{\text{age.edu}} \sim \mathcal{N}\left(0 \,,\, \sigma_{\text{age.edu}}\right) \text{ for } k = 1, \ldots, K, l = 1, \ldots, L$$

$$\alpha_m^{\text{region}} \sim \mathcal{N}\left(0 \,,\, \sigma_{\text{region}}\right) \text{ for } m = 1, \ldots, M.$$

The standard deviation terms all have uniform hyper-priors, constrained between 0 and 100.

H   Non-negative Matrix Factorization: Constrained Gamma Poisson Model

The Gamma Poisson factorization model describes discrete data matrices [11, 12].

Consider a $U \times I$ matrix of observations. We find it helpful to think of $u = \{1, \cdots, U\}$ as users and $i = \{1, \cdots, I\}$ as items, as in a recommendation system setting. The generative process for a Gamma Poisson model with K factors is

1. For each user u in $\{1, \cdots, U\}$:
   - For each component k, draw $\theta_{uk} \sim \mathrm{Gam}(a_0, b_0)$.
2. For each item i in $\{1, \cdots, I\}$:
   - For each component k, draw $\beta_{ik} \sim \mathrm{Gam}(c_0, d_0)$.
3. For each user and item:
   - Draw the observation $y_{ui} \sim \mathrm{Poisson}(\boldsymbol{\theta}_u^\top \boldsymbol{\beta}_i)$.

A potential downfall of this model is that it is not uniquely identifiable: swapping rows and columns of $\boldsymbol{\theta}$ and $\boldsymbol{\beta}$ give the same inner product. One way to contend with this is to constrain either vector to be an ordered vector during inference. We constrain each $\boldsymbol{\theta}_u$ vector in our model in this fashion. Stan code is in Figure 8. We set $K = 10$ and all the Gamma hyper-parameters to 1 in our experiments.

I   Non-negative Matrix Factorization: Dirichlet Exponential Model

Another model for discrete data is a Dirichlet Exponential model. The Dirichlet enforces uniqueness while the exponential promotes sparsity. This is a non-conjugate model that does not appear to have been studied in the literature.

The generative process for a Dirichlet Exponential model with K factors is

1. For each user u in $\{1, \cdots, U\}$:
   - Draw the K-vector $\boldsymbol{\theta}_u \sim \mathrm{Dir}(\boldsymbol{\alpha}_0)$.
2. For each item i in $\{1, \cdots, I\}$:
   - For each component k, draw $\beta_{ik} \sim \mathrm{Exponential}(\lambda_0)$.
3. For each user and item:
   - Draw the observation $y_{ui} \sim \mathrm{Poisson}(\boldsymbol{\theta}_u^\top \boldsymbol{\beta}_i)$.

Stan code is in Figure 9. We set $K = 10$, $\alpha_0 = 1000$ for each component, and $\lambda_0 = 0.1$. With this configuration of hyper-parameters, the factors $\boldsymbol{\beta}_i$ appear sparse.

J   Gaussian Mixture Model

The Gaussian mixture model (GMM) is a celebrated probability model. We use it to group a dataset of natural images based on their color histograms. We build a high-dimensional GMM with a Gaussian prior for the mixture means, a lognormal prior for the mixture standard deviations, and a Dirichlet prior for the mixture components.

The images are in $\mathbf{Y} = \boldsymbol{y}_{1:N}$ where each $\boldsymbol{y}_n$ is D-dimensional and there are N observations. The likelihood for the images is

$$p(\mathbf{Y} \mid \boldsymbol{\theta}, \boldsymbol{\mu}, \boldsymbol{\sigma}) = \prod_{n=1}^{N} \sum_{k=1}^{K} \theta_k \prod_{d=1}^{D} \mathcal{N}(y_{nd} \mid \mu_{kd}, \sigma_{kd})$$

with a Dirichlet prior for the mixture proportions

$$p(\boldsymbol{\theta}) = \mathrm{Dir}(\boldsymbol{\theta} \, ; \, \boldsymbol{\alpha}_0),$$

a Gaussian prior for the mixture means

$$p(\boldsymbol{\mu}) = \prod_{k=1}^{D} \prod_{d=1}^{D} \mathcal{N}(\mu_{kd} \,;\, 0, 1)$$

and a lognormal prior for the mixture standard deviations

$$p(\boldsymbol{\sigma}) = \prod_{k=1}^{D} \prod_{d=1}^{D} \text{logNormal}(\sigma_{kd} \,;\, 0, 1)$$

The dimension of the color histograms in the imageCLEF dataset is $D = 576$. This is a concatenation of three 192-length histograms, one for each color channel (red, green, blue) of the images.

We scale the image histograms to have zero mean and unit variance. Setting α_0 to a small value encourages the model to use fewer components to explain the data. Larger values of α_0 encourage the model to use all K components. We set $\alpha_0 = 1\,000$ in our experiments.

ADVI code is in Figure 10. The stochastic data subsampling version of the code is in Figure 11.

```
data {
  int<lower=0> N;    // number of data items
  int<lower=0> D;    // dimension of input features
  matrix[N,D]  x;    // input matrix
  vector[N]    y;    // output vector

  // hyperparameters for Gamma priors
  real<lower=0> a0;
  real<lower=0> b0;
  real<lower=0> c0;
  real<lower=0> d0;
}

parameters {
  vector[D] w;                // weights (coefficients) vector
  real<lower=0> sigma;        // standard deviation
  vector<lower=0>[D] alpha;   // hierarchical latent variables
}

transformed parameters {
  vector[D] one_over_sqrt_alpha;
  for (i in 1:D) {
    one_over_sqrt_alpha[i] <- 1 / sqrt(alpha[i]);
  }
}

model {
  // alpha: hyper-prior on weights
  alpha ~ gamma(c0, d0);

  // sigma: prior on standard deviation
  sigma ~ inv_gamma(a0, b0);

  // w: prior on weights
  w ~ normal(0, sigma * one_over_sqrt_alpha);

  // y: likelihood
  y ~ normal(x * w, sigma);
}
```

Figure 6: Stan code for Linear Regression with Automatic Relevance Determination.

```stan
data {
  int<lower=0> N;
  int<lower=0> n_age;
  int<lower=0> n_age_edu;
  int<lower=0> n_edu;
  int<lower=0> n_region_full;
  int<lower=0> n_state;
  int<lower=0,upper=n_age> age[N];
  int<lower=0,upper=n_age_edu> age_edu[N];
  vector<lower=0,upper=1>[N] black;
  int<lower=0,upper=n_edu> edu[N];
  vector<lower=0,upper=1>[N] female;
  int<lower=0,upper=n_region_full> region_full[N];
  int<lower=0,upper=n_state> state[N];
  vector[N] v_prev_full;
  int<lower=0,upper=1> y[N];
}
parameters {
  vector[n_age] a;
  vector[n_edu] b;
  vector[n_age_edu] c;
  vector[n_state] d;
  vector[n_region_full] e;
  vector[5] beta;
  real<lower=0,upper=100> sigma_a;
  real<lower=0,upper=100> sigma_b;
  real<lower=0,upper=100> sigma_c;
  real<lower=0,upper=100> sigma_d;
  real<lower=0,upper=100> sigma_e;
}
transformed parameters {
  vector[N] y_hat;

  for (i in 1:N)
    y_hat[i] <- beta[1]
                + beta[2] * black[i]
                + beta[3] * female[i]
                + beta[5] * female[i] * black[i]
                + beta[4] * v_prev_full[i]
                + a[age[i]]
                + b[edu[i]]
                + c[age_edu[i]]
                + d[state[i]]
                + e[region_full[i]];
}
model {
  a ~ normal (0, sigma_a);
  b ~ normal (0, sigma_b);
  c ~ normal (0, sigma_c);
  d ~ normal (0, sigma_d);
  e ~ normal (0, sigma_e);
  beta ~ normal(0, 100);
  y ~ bernoulli_logit(y_hat);
}
```

Figure 7: Stan code for Hierarchical Logistic Regression, from [10].

```
data {
  int<lower=0> U;
  int<lower=0> I;
  int<lower=0> K;
  int<lower=0> y[U,I];
  real<lower=0> a;
  real<lower=0> b;
  real<lower=0> c;
  real<lower=0> d;
}

parameters {
  positive_ordered[K] theta[U]; // user preference
  vector<lower=0>[K] beta[I];   // item attributes
}

model {
  for (u in 1:U)
    theta[u] ~ gamma(a, b); // componentwise gamma
  for (i in 1:I)
    beta[i] ~ gamma(c, d);  // componentwise gamma

  for (u in 1:U) {
    for (i in 1:I) {
      y[u,i] ~ poisson(theta[u]'*beta[i]);
    }
  }
}
```

Figure 8: Stan code for Gamma Poisson non-negative matrix factorization model.

```
data {
  int<lower=0> U;
  int<lower=0> I;
  int<lower=0> K;
  int<lower=0> y[U,I];
  real<lower=0> lambda0;
  real<lower=0> alpha0;
}

transformed data {
  vector<lower=0>[K] alpha0_vec;
  for (k in 1:K) {
    alpha0_vec[k] <- alpha0;
  }
}

parameters {
  simplex[K] theta[U];          // user preference
  vector<lower=0>[K] beta[I];   // item attributes
}

model {
  for (u in 1:U)
    theta[u] ~ dirichlet(alpha0_vec); // componentwise dirichlet
  for (i in 1:I)
    beta[i] ~ exponential(lambda0);   // componentwise exponential

  for (u in 1:U) {
    for (i in 1:I) {
      y[u,i] ~ poisson(theta[u]'*beta[i]);
    }
  }
}
```

Figure 9: Stan code for Dirichlet Exponential non-negative matrix factorization model.

```
data {
  int<lower=0> N;          // number of data points in entire dataset
  int<lower=0> K;          // number of mixture components
  int<lower=0> D;          // dimension
  vector[D] y[N];          // observations

  real<lower=0> alpha0;  // dirichlet prior
}

transformed data {
  vector<lower=0>[K] alpha0_vec;
  for (k in 1:K)
    alpha0_vec[k] <- alpha0;
}

parameters {
  simplex[K] theta;                      // mixing proportions
  vector[D] mu[K];                       // locations of mixture components
  vector<lower=0>[D] sigma[K];  // standard deviations of mixture components
}

model {
  // priors
  theta ~ dirichlet(alpha0_vec);
  for (k in 1:K) {
      mu[k] ~ normal(0.0, 1.0);
      sigma[k] ~ lognormal(0.0, 1.0);
  }

  // likelihood
  for (n in 1:N) {
    real ps[K];
    for (k in 1:K) {
      ps[k] <- log(theta[k]) + normal_log(y[n], mu[k], sigma[k]);
    }
    increment_log_prob(log_sum_exp(ps));
  }
}
```

Figure 10: Stan code for the GMM example.

```
functions {
  real divide_promote_real(int x, int y) {
    real x_real;
    x_real <- x;
    return x_real / y;
  }
}

data {
  int<lower=0> NFULL;        // total number of datapoints in dataset
  int<lower=0> N;            // number of data points in minibatch

  int<lower=0> K;            // number of mixture components
  int<lower=0> D;            // dimension

  vector[D] yFULL[NFULL];    // dataset
  vector[D] y[N];            // minibatch

  real<lower=0> alpha0;      // dirichlet hyper-prior parameter
}

transformed data {
  real minibatch_factor;
  vector<lower=0>[K] alpha0_vec;
  for (k in 1:K) {
    alpha0_vec[k] <- alpha0 / K;
  }
  minibatch_factor <- divide_promote_real(N, NFULL);
}

parameters {
  simplex[K] theta;                      // mixing proportions
  vector[D] mu[K];                       // locations of mixture components
  vector<lower=0>[D] sigma[K];           // standard deviations of mixture components
}

model {
  // priors
  theta ~ dirichlet(alpha0_vec);
  for (k in 1:K) {
      mu[k] ~ normal(0.0, 1.0);
      sigma[k] ~ lognormal(0.0, 1.0);
  }

  // likelihood
  for (n in 1:N) {
    real ps[K];
    for (k in 1:K) {
      ps[k] <- log(theta[k]) + normal_log(y[n], mu[k], sigma[k]);
    }
    increment_log_prob(log_sum_exp(ps));
  }
  increment_log_prob(log(minibatch_factor));
}
```

Figure 11: Stan code for the GMM example, with stochastic subsampling of the dataset.

References

[1] Erhan Çınlar. *Probability and Stochastics*. Springer, 2011.

[2] David J Olive. *Statistical Theory and Inference*. Springer, 2014.

[3] John Duchi, Elad Hazan, and Yoram Singer. Adaptive subgradient methods for online learning and stochastic optimization. *The Journal of Machine Learning Research*, 12:2121–2159, 2011.

[4] T Tieleman and G Hinton. Lecture 6.5-rmsprop: Divide the gradient by a running average of its recent magnitude. *COURSERA: Neural Networks for Machine Learning*, 4, 2012.

[5] Diederik Kingma and Jimmy Ba. Adam: A method for stochastic optimization. *arXiv preprint arXiv:1412.6980*, 2014.

[6] Matthew D Hoffman, David M Blei, Chong Wang, and John Paisley. Stochastic variational inference. *The Journal of Machine Learning Research*, 14(1):1303–1347, 2013.

[7] Christopher M Bishop. *Pattern Recognition and Machine Learning*. Springer New York, 2006.

[8] Jan Drugowitsch. Variational Bayesian inference for linear and logistic regression. *arXiv preprint arXiv:1310.5438*, 2013.

[9] Andrew Gelman and Jennifer Hill. *Data analysis using regression and multilevel/hierarchical models*. Cambridge University Press, 2006.

[10] Stan Development Team. *Stan Modeling Language Users Guide and Reference Manual*, 2015.

[11] John Canny. GaP: a factor model for discrete data. In *ACM SIGIR*, pages 122–129. ACM, 2004.

[12] Ali Taylan Cemgil. Bayesian inference for nonnegative matrix factorisation models. *Computational Intelligence and Neuroscience*, 2009, 2009.